

PHYSICAL REVIEW C

NUCLEAR PHYSICS

THIRD SERIES, VOL. 5, NO. 2

February 1972

Structure of Mass 15: The $^{14}\text{N}(p, \gamma)^{15}\text{O}$ and $^{14}\text{N}(p, p'\gamma)$ Reactions*

G. W. Phillips,† Patrick Richard, D. O. Elliott, F. F. Hopkins, and A. C. Porter‡

Center for Nuclear Studies, The University of Texas, Austin, Texas 78712

(Received 29 September 1971)

We have studied states in ^{15}O between 10.91- and 13.02-MeV excitation as resonances in the $^{14}\text{N}(p, \gamma)^{15}\text{O}$ and $^{14}\text{N}(p, p'\gamma)$ reactions. Several new states are reported, and the elastic, inelastic, and γ -ray partial widths are given for some of the levels. The levels are compared with corresponding levels in the mirror nucleus ^{15}N . Of particular interest are the $\frac{1}{2}^+$ and $\frac{5}{2}^+$, $T = \frac{3}{2}$ states which should lie in this region. The results imply more mixing of these states in ^{15}O with nearby $T = \frac{1}{2}$ levels than is observed in ^{15}N . However, most of the $T = \frac{3}{2}$ strength in ^{15}O remains unaccounted for.

I. INTRODUCTION

The mirror symmetry of levels in ^{15}N and ^{15}O is well established up to about 10 MeV in excitation. With few exceptions, the experimentally observed levels in the two nuclei can be matched up one-to-one with respect to spin, parity, and other measurable properties such as γ -decay strength and branching ratios.¹⁻⁴

At higher energies, the level structure in ^{15}N between 11 and 13 MeV has been investigated in detail by observing resonances in the $^{14}\text{C} + p$ and $^{14}\text{N} + n$ reactions.⁴⁻⁶ The corresponding region in ^{15}O was first investigated via the reaction $^{14}\text{N}(p, p'\gamma)^{14}\text{N}$.⁷ More recently, West *et al.*⁸ have reported measurements of elastic and inelastic scattering of protons on ^{14}N , in which a number of resonances were observed in the compound nucleus ^{15}O between 10.9- and 12.5-MeV excitation energy. However, the observed levels in this region could not be so readily compared between ^{15}N and ^{15}O as could the lower excited states.

Strong γ -ray transitions have been observed from the $T = \frac{3}{2}$ levels in ^{15}N at 11.61 and 12.52 MeV.⁶⁻¹⁰ In the present experiment, we have studied the γ decay of resonances in ^{15}O from the $^{14}\text{N} + p$ reactions at proton energies from 3.9 to 5.3 MeV (10.9- to 12.2-MeV excitation energy in ^{15}O). γ -decay widths and branching ratios are reported.

We have also measured inelastic proton cross sections leading to the first and second excited states in ^{14}N , up to an incident proton energy of 6.4 MeV, by observing γ rays from the $^{14}\text{N}(p, p'\gamma)$ reaction.

II. PROCEDURE

Nitrogen targets were prepared by evaporating melamine ($\text{C}_3\text{H}_6\text{N}_6$) onto thin carbon backings. These were positioned in a small (4-in. cube) aluminum scattering chamber with Plexiglass windows for the γ -ray detectors on each side of the beam line. The proton beam from the EN tandem Van de Graaff accelerator at the Center for Nuclear Studies of The University of Texas at Austin was focused on target through a $\frac{3}{8}$ -in.-diam tantalum collimator and collected behind the target in a beam dump which was shielded from the detectors by a concrete wall. Excitation curves for proton energies from 3.75 to 5.22 MeV were taken simultaneously for ground-state γ rays following proton capture by ^{14}N (Fig. 1, top) and for the 2.31-MeV γ rays following inelastic scattering to the first excited state of ^{14}N (Fig. 1, bottom). The former was taken with a 4-in. \times 4-in. NaI detector at a distance of 3 in. from the target, and an angle of 90° on one side of the beam line, and the latter with a 30-cm³ coaxial Ge(Li) detector placed symmetrically on the other side. The curves are nor-

malized to an inelastic cross section of 61 mb for the state at 3.90 MeV, as given in Ref. 8. Systematic uncertainty in this normalization is estimated at less than 10% for the $(p, p'\gamma)$ curve and less than 20% for the (p, γ_0) curve. The latter is due mainly to uncertainty in the relative detector efficiency with energy (see Sec. III). There is additional uncertainty in the (p, γ_0) curve due to the possible effects of non-isotropic angular distributions; however, the large solid angle covered by the detector serves to minimize these effects. Because the 2.31-MeV level of ^{14}N has zero spin, its decay should be isotropic and the $(p, p'\gamma)$ curve at 90° truly reflects the total cross section.

Portions of the $^{14}\text{N}(p, p'\gamma)$ curve were repeated later in finer steps to better define and resolve the overlapping resonances observed, and the curve was extended to a proton energy of 6.36 MeV (Fig. 2, top). This covers the gap between 5.67 MeV, where the data of West *et al.*⁸ end, and 6.0 MeV, where the inelastic proton cross-section

measurements by Shrivastava, Boreli, and Kinsey¹¹ begin. In this region the p_2 inelastic cross section becomes appreciable to the second excited state of ^{14}N at 3.95 MeV which decays 96% of the time via a 1.64-MeV cascade γ ray to the first excited state. The excitation curve for this γ ray is

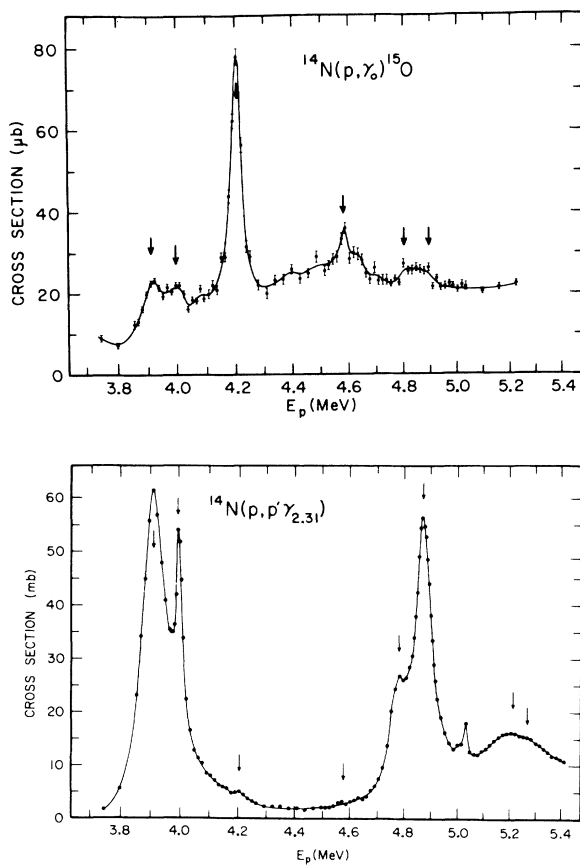


FIG. 1. Excitations for $^{14}\text{N} + p$ for $E_p = 3.7$ to 5.5 MeV. The γ_0 resonance decay (to the ^{15}O ground state) is given in the top figure and the $(p, p'\gamma_{2.31})$ resonance decay (through the ^{14}N 2.31-MeV level) is given in the lower figure.

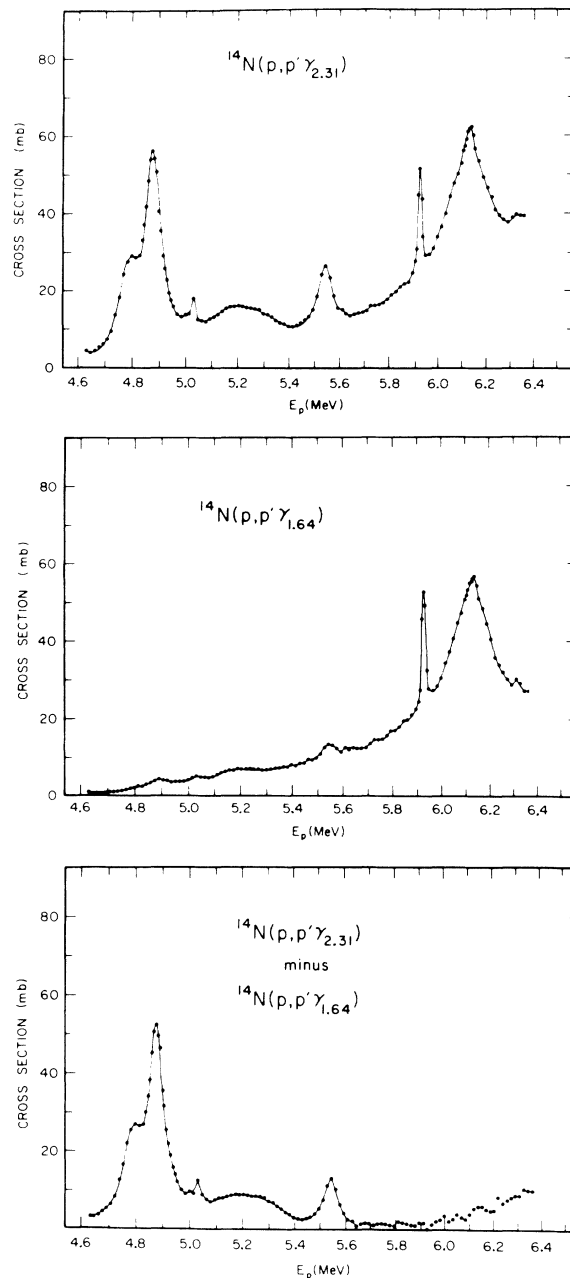


FIG. 2. Excitation functions for the $^{14}\text{N}(p, p'\gamma)$ reaction for E_p from 4.6 to 6.4 MeV for $E_\gamma = 2.31$ and $E_\gamma = 1.64$ MeV. The lowest curve is the difference in the two excitation functions, which corrects for the γ -ray cascading of the ^{14}N 3.95-MeV state through the first excited state at 2.31 MeV.

shown in Fig. 2, center. Because this γ ray feeds the 2.31-MeV level, the curve for the 2.31-MeV γ ray represents the sum of the p_1 cross section plus 0.96 times the p_2 cross section. To approximate the p_1 cross section, the excitation curve for the 1.64-MeV γ ray, normalized by the relative detection efficiencies, is subtracted from the curve for the 2.31-MeV γ ray (Fig. 2, bottom). However, since the 1.64-MeV γ ray may have a non-isotropic angular distribution, its curve should rightly be considered as 4π times the cross section at 90° . Where they overlap, there is good over-all agreement between the present data and the inelastic cross sections measured by Shrivastava, Boreli, and Kinsey,¹¹ although the latter data are much less detailed than the present work. Table I summarizes the present results.

To obtain branching ratios for γ decay of the resonances observed in Fig. 1, pulse-height spectra from the Ge(Li) detector were accumulated at the positions indicated by arrows on the figure. The resulting spectra are shown in Figs. 3–5. Off-resonance spectra were also taken at 4.10 and 4.70 MeV. These confirmed the sizable direct-capture cross section to the ^{15}O ground state, seen in Fig. 1, and also showed appreciable direct capture to the 6.79-MeV level.

III. RESULTS

Table I gives the resonance energies E_p , excitation energies E_x , total widths Γ , elastic and inelastic partial widths Γ_0 and Γ_1 , and gamma widths Γ_γ for the levels seen in the present experiment. These are compared with levels in the correspond-

ing region of ^{15}N in Table II.

Total widths were obtained from a computer fit to the data using a background term plus one or two Breit-Wigner resonance shapes including interference terms (see the work of Wharton *et al.*¹²). Partial widths were obtained from the inelastic peak cross sections, which are proportional to $\Gamma_0\Gamma_1/\Gamma$ (see e.g., Ref. 8). If there are no other significant channels, $\Gamma_0 = \Gamma - \Gamma_1$, and this gives a quadratic equation that can be solved for Γ_1 . However, there is generally an ambiguity as to which root to choose for Γ_1 (the other root is then Γ_0). In the present case, we have additional information in the (p, γ_0) resonant cross sections which are proportional to $\Gamma_0\Gamma_\gamma/\Gamma$. The choice of the larger root for Γ_1 and the smaller root for Γ_0 in most cases gave unreasonably large γ widths and so could be eliminated. An exception is the 10.94-MeV level, for which the two roots are close in value. Here we follow the lead of West *et al.*,⁸ who were guided by the elastic cross section in choosing the larger root for Γ_1 . Where they overlap, there is good agreement between the present experiment and that of Ref. 8 in resonance energies and widths. Also given in Table II are the reduced widths

$$\gamma_T^2 = \Gamma_T/2P_l,$$

where Γ_T is the partial width for decay to a mass-14 state with isospin T , and the P_l are the Coulomb penetrability functions for angular momentum transfer l . The reduced widths are normalized for comparison between ^{15}O and ^{15}N by dividing by c^2 , the square of the isospin vector coupling coef-

TABLE I. ^{15}O levels from $^{14}\text{N}(p, p'\gamma)$ and $^{14}\text{N}(p, \gamma)$.

E_p^a (MeV)	E_x^a (MeV)	Γ^b (keV)	Γ_0^b (keV)	Γ_1^c (keV)	Γ_2^c (keV)	Γ_γ (eV)
3.903	10.936	99	39	60		14 ± 3
3.996	11.023	25	21	4		1.4 ± 0.4
4.203	11.216	40 ± 4	40 ± 4			5.2 ± 0.4
4.58	11.57	20 ± 15	20 ± 15			0.7 ± 0.2
4.63	11.61	80 ± 50	80 ± 50			
4.772	11.747	99	95	4		
4.877	11.845	65	60	5		
5.03	11.99	20 ± 5	20 ± 5	0.2 ± 0.1		
5.18	12.12	200 ± 50	200 ± 50	3 ± 1		
5.28	12.22	100 ± 50		wk.		
5.547	12.467	77		1.3 ± 0.4	0.4 ± 0.1	
5.937	12.831	16			str.	
6.123	13.004	215 ± 30			str.	
6.141	13.022	40 ± 30			str.	

^a Uncertainty of 3 keV (20 keV) in energies given to 1 (10) keV.

^b Uncertainty of <5% unless given otherwise.

^c wk., observed weakly; str., observed strongly.

ficient for the respective decay channel.

Table III gives the γ -ray total cross sections, resonant cross sections, branching ratios, and γ widths obtained for resonances at 3.90, 4.00, 4.58, 4.78, and 4.87 MeV, and compares these with the single-particle widths in Weiskopf units (W.u.), assuming the lowest allowed multipolarity as given in the table.

The $^{14}\text{N}(p, \gamma_0)$ cross sections can be compared with recently published data of Kuan *et al.*,¹³ who obtained $^{14}\text{N}(p, \gamma_0)$ cross sections at 90° , including the region covered in the present work, but in less detail. The over-all relative agreement is good, although in Ref. 13 the resonance at 4.00 MeV is not resolved from the 3.90-MeV resonance. However, the absolute cross section obtained in the present work exceeds that of Ref. 13 by approximately a factor of 2. This disagreement is disturbing; however, there are several checks on the absolute cross sections obtained here. In the following, we present in some detail the procedures used in obtaining these cross sections:

(1) The $^{14}\text{N}(p, \gamma_0)$ cross section was determined relative to a value of 61 mb for the $^{14}\text{N}(p, p'\gamma)$ cross section at the 3.90-MeV resonance, as obtained by West *et al.*,⁸ using peak and total efficiencies interpolated from Marion and Young.¹⁴ The γ_0 energies ranged from approximately 10.9 to 12.0 MeV. Counts were summed in a moving window centered on the incompletely resolved full-energy, first-escape, and second-escape peaks in the spectrum, and a flat background from above the window was subtracted. The efficiency ratio of counts in the window to total counts was extracted from the spectra with the greatest number of counts, i.e., at the 4.20-MeV resonance.

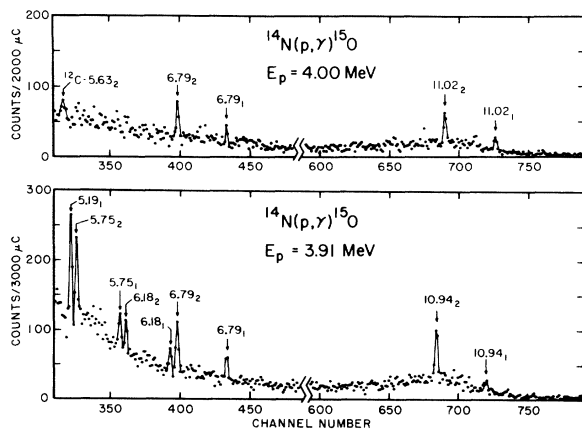


FIG. 3. High-energy $^{14}\text{N}(p, \gamma)^{15}\text{O}$ γ -ray spectra taken with a Ge(Li) detector nominally 33-cm³ active volume. Energies are in MeV. Subscripts 0, 1, and 2 identify full-energy, single-escape, and double-escape peaks, respectively.

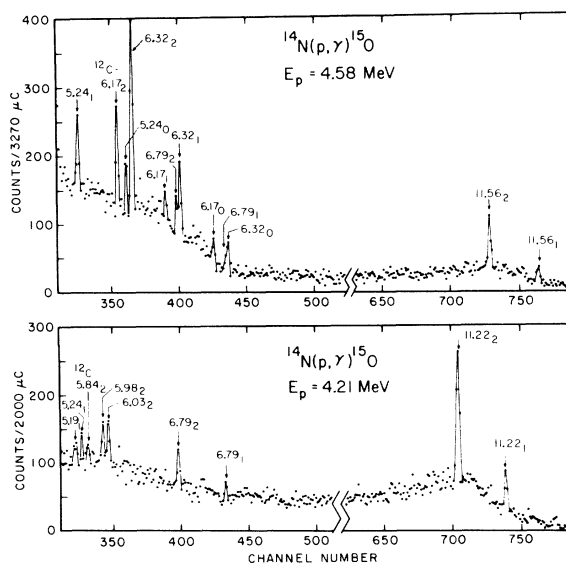


FIG. 4. See Fig. 3 caption.

To obtain this ratio, the flat Compton scattering region below the window was extrapolated to zero energy underneath the peaks from lower-energy γ rays. It was assumed that this peak-to-Compton efficiency ratio did not change appreciably over the region studied.

(2) The spectra of high-energy γ rays (Figs. 3–5) taken with the Ge(Li) detector provide an independent check at several energies of the γ_0 cross section relative to the $^{14}\text{N}(p, p'\gamma)$ cross section. Using relative efficiencies extrapolated from Ref. 14 and normalizing to the 3.90-MeV resonance, we obtained the results given in column 5 of Table III.

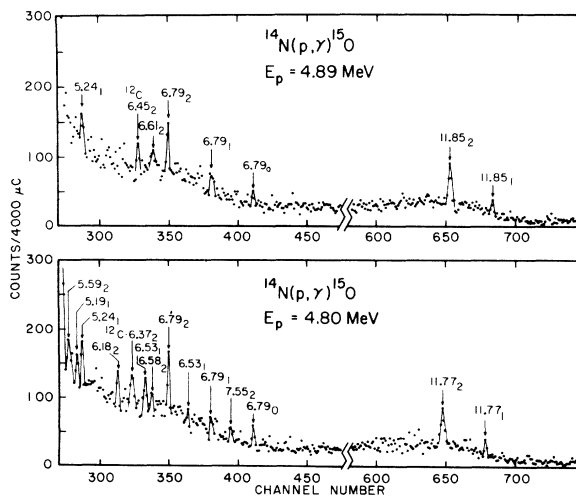


FIG. 5. See Fig. 3 caption.

TABLE II. Comparison of levels in ^{15}O and ^{15}N .

E_x (MeV)	$J^\pi; T^a$	l_0^d	^{15}O					Γ_γ (eV)
			Γ_0 (keV)	γ_0^2/c^2 (keV)	l_1^e	Γ_1 (keV)	γ_1^2/c^2 (keV)	
Negative parity								
11.02	$\frac{1}{2}^-$	1	21	10	1	4	33	1.4
11.57	$\frac{5}{2}^-$	1	25	10				0.3
11.61	$(\frac{1}{2}, \frac{3}{2})^-$	1	25	10				
11.85	$(\frac{5}{2}^-)$	1	60	22	1	5	15	
11.99	$\frac{5}{2}^-$	1	20	7				
12.47	$(\frac{3}{2}, \frac{5}{2})^-$	1	58	19	1	2	3	
Positive parity								
10.91	$\frac{7}{2}^+$	2	90	105				
10.94	$\frac{1}{2}^+; \frac{1}{2}^+$	0	39	14	0	60	213 107	14
11.22	$\frac{3}{2}^+$	2	40	40				5
11.75	$\frac{5}{2}^+; \frac{1}{2}^+$	2	95	75	2	4	51 25	
12.12	$\frac{5}{2}^+$	2	160	105	(2)	3	30	
E_x (MeV)	$J^\pi; T^a$	l_0^b	^{15}N					Γ_γ (eV)
			Γ_0 (keV)	γ_0^2/c^2 (keV)	l_1^c	Γ_1 (keV)	γ_1^2/c^2 (keV)	
Negative parity								
11.29	$\frac{1}{2}^-$	1	2	4	1	6	35	0.3
11.88	$(\frac{3}{2}, \frac{5}{2})^-$	1	25	22	3	0.03	5	
11.96	$\frac{1}{2}^-$	1	21	17	1	0.3	0.6	
12.14	$\frac{3}{2}^-$	1	30	21	1	17	27	
12.32	$\frac{5}{2}^-$	(1)	21	12	(1)	0.3	0.5	
12.92	$\frac{3}{2}^-$	1	39	18				
Positive parity								
11.24	$\geq \frac{3}{2}$	≥ 1	<3	<580 ($l=2$)				
11.42	$\frac{1}{2}^+$	0	23	14	0	11	18	4
11.56	$\frac{1}{2}^+; \frac{3}{2}^+$	0	4	2	0	400	1140	19
11.76	$\frac{3}{2}^+$	0	37	18	0	0.5	0.6	
12.09	$\frac{5}{2}^+$	2	12	50	2	2	17	
12.49	$(\frac{3}{2}^+)$	2	28	56	2	0.3	1	
12.52	$\frac{5}{2}^+; \frac{3}{2}^+$				2	80	720	

^a $T = \frac{1}{2}$ if not stated.

^b $^{14}\text{N}+n$, Refs. 4 and 5.

^c $^{14}\text{C}+p$, Refs. 4 and 5.

^d $^{14}\text{N}(\text{g.s.})+p_0$, Refs. 8, 13, and present work.

^e $^{14}\text{N}^*(2.31)+p_1$, Refs. 8, 13, and present work.

Agreement with the curve of Fig. 1 is generally satisfactory.

(3) An additional check of the normalization is provided by the $^{14}\text{N}(p, p'\gamma_{1,64})$ curve (Fig. 2) and the $^{14}\text{N}(p, p'\gamma_{2,31})$ minus the $^{14}\text{N}(p, p'\gamma_{1,64})$ curve (Fig. 2). Above 6 MeV these can be compared with the inelastic cross sections¹¹ for the first and second excited states. Again agreement is satisfactory.

Thus, the relative cross-section measurements, taken independently and at different times with the NaI detector and the Ge(Li) detector, are consistent. In addition, the present data bridge the gap between the absolute measurements of the inelastic scattering cross sections made in Refs. 8 and 11 at different energies and are consistent with both these measurements. This gives us confidence in the absolute normalization obtained for the present work.

IV. DISCUSSION

A. Low-Lying Levels in Mass-15 Nuclei

Figure 6 compares the level structure of the mass-15 nuclei⁴ up to and including the region of excitation studied in the present work. There is very good agreement in level spacings, spins and parities, and properties such as γ -ray branching and relative stripping cross sections, at least up

to the proton separation energy at 7.29 MeV in ^{15}O , and good general agreement up to about 10 MeV in excitation. Figure 7 compares γ branching ratios between mirror levels in ^{15}N and ^{15}O .^{1-3,15} There is serious disagreement for the two pairs of $\frac{1}{2}^+$ levels at 7.55, 8.31, and 8.79, 9.05 MeV in ^{15}O , ^{15}N , respectively. In both cases the $E1$ ground-state decay, relative to the $E1$ decay to the $\frac{3}{2}^-$ third excited state and to the competing $M1$ decays, is severely inhibited in ^{15}O . This represents a breakdown in mirror symmetry and has been discussed previously,^{1,3} but is still not well understood. Except for this situation, the agreement between branching ratios in mirror levels is very good up to 10 MeV. The data indicate that a missing level at about 9 MeV in ^{15}O (the mirror of the 9.155-MeV level in ^{15}N) may be part of an unresolved doublet at 8.92 MeV, the other member of the doublet being the mirror of the 9.23-MeV level in ^{15}N . There is recent experimental evidence that this may be the case.¹⁶ The branching-ratio data also indicate that the 9.93-MeV level in ^{15}N is the mirror of the $\frac{3}{2}^-$ 9.61-MeV level in ^{15}O . The ^{15}N level was previously assigned positive parity on evidence which has proven unreliable¹⁵ in the case of the 9.76-MeV level in ^{15}N . Recent experiments¹⁶ have given additional information about the 10–11-MeV region in ^{15}O which is not included in Fig. 6.

TABLE III. $^{14}\text{N}(p, \gamma)^{15}\text{O}$ decay properties.

E_{res} (MeV)	J^π	E_f (MeV)	E_γ (MeV)	Cross section		Branching ratio (%)	Γ_γ (eV)	Multipolarity	$\Gamma_\gamma/\Gamma_{s, p.}$ (W.u.)
				Total (μb)	Resonant (μb)				
3.91	$\frac{1}{2}^+$	0	10.94	21 \pm 3	14 \pm 4	44 \pm 8	14 \pm 4	$E1$	0.026
		5.18	5.76	11 \pm 2	11 \pm 2	34 \pm 3	11 \pm 2	$M1$	3.
		6.18	6.18 ^a	7 \pm 2	7 \pm 2	22 \pm 8	7 \pm 2	$E1$	0.16
		6.79	6.79 ^a	10 \pm 2	<3	<8	<3	$M1$	
4.00	$\frac{1}{2}^-$	0	11.02	20 \pm 3	12 \pm 4	100	1.4 \pm 0.4	$M1$	0.05
		6.79	6.79 ^a	10 \pm 3	<4	<25	<0.4	$E1$	
4.20	$\frac{3}{2}^+$	0	11.22	82 \pm 6	64 \pm 6	74 \pm 5	5.5 \pm 0.5	$E1$	0.009
		5.18	6.04	12 \pm 2	12 \pm 2	14 \pm 5	1.0 \pm 0.2	$M1$	0.02
		5.24	5.98	10 \pm 2	10 \pm 2	12 \pm 5	0.9 \pm 0.2	$M1$	0.2
		6.79	6.79 ^a	11 \pm 2	<4	<4	<0.4	$M1$	
4.58	$\frac{5}{2}^-$	0	11.57	26 \pm 3	8 \pm 4	18 \pm 9	0.3 \pm 0.2	$E2$	0.07
		5.24	6.33	30 \pm 3	30 \pm 3	63 \pm 9	1.2 \pm 0.1	$E1$	0.012
		6.18	6.18 ^a	10 \pm 4	10 \pm 4	20 \pm 9	0.4 \pm 0.2	$M1$	0.12
		6.79	6.79 ^a	6 \pm 2	<1	<3	<0.1	$E1$	
4.78	$\frac{5}{2}^+$	0	11.75	24 \pm 3	<7	<30		$M2$	
		5.18	6.57	<5	<5	<25		$E2$	
		5.24	6.51	8 \pm 1	8 \pm 1	47 \pm 7	5 \pm 1	$M1$	0.09
		6.18	5.57	9 \pm 2	9 \pm 2	53 \pm 7	5 \pm 1	$E1$	0.07
		6.79	6.79 ^a	11 \pm 2	<4	<20		$M1$	
4.87	$\frac{5}{2}^-$	11.84	0	22 \pm 3	<5	<50		$M2$	
		5.24	6.60	5 \pm 2	5 \pm 2	100	1.4 \pm 0.6	$E1$	0.012
		6.79	6.79 ^a	11 \pm 2	<4	<40		$E1$	

^aCascade γ ray observed.

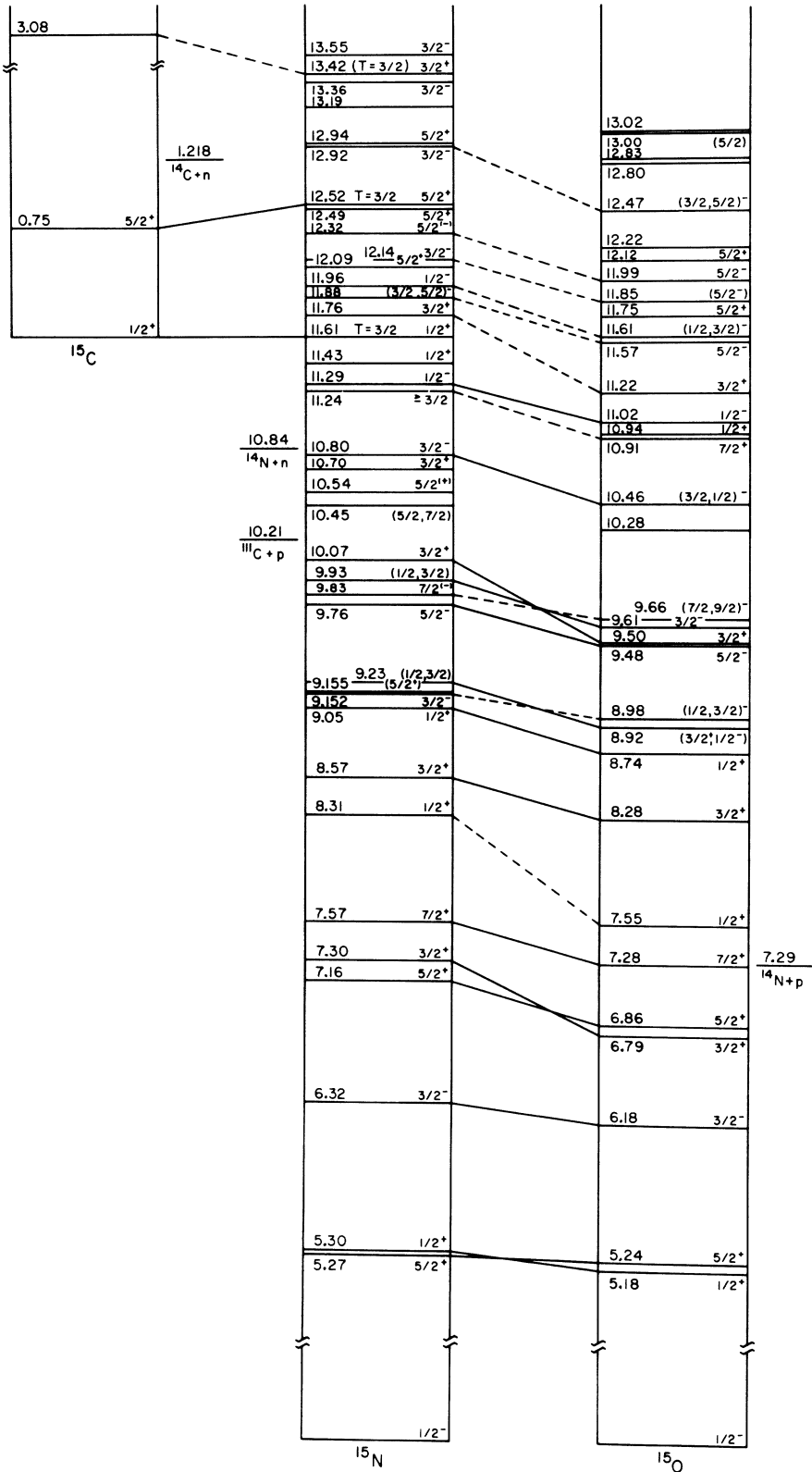


FIG. 6. Level structure for mass-15 nuclei.

There have been a number of theoretical calculations of level structure in mass 15 up to about 10 MeV based on the individual-particle model (IPM) (see e.g., the works of Halbert and French¹⁷ and Zucher, Buck, and McGrory¹⁸) and on the weak-coupling model (WCM).^{19,20} The consensus of the theoretical and experimental evidence is that the $\frac{1}{2}^-$ ground state and $\frac{3}{2}^-$ third excited state are primarily $p_{1/2}$ and $p_{3/2}$ holes in the ^{16}O closed shell. The positive-parity levels below 8.6 MeV can be well described as an excitation of one particle into the $2s_{1/2}$ or $1d_{5/2}$ subshells leaving two holes in the $1p$ core. Evidence from the (d, p) stripping reaction³ and ^{15}C β decay²¹ show strengths to these levels of nearly single-particle intensity, exceeding the theoretical strengths calculated from the IPM. There is, however, some mixing of the $\frac{1}{2}^+$ single-particle strength²² expected for the 5.30-MeV level into the 9.05-MeV level in ^{15}N , and of the $\frac{3}{2}^+$ strength²³ expected for the 8.57-MeV level into the 10.07-MeV level in ^{15}N .

B. Levels Between 9 and 10 MeV

There are two interesting sets of levels of opposite parity intermixed between 9.05 and 10.07 MeV in ^{15}N . The relative positions and γ -decay properties of the positive-parity levels are well reproduced in the WCM calculations of Lie and Engeland,²⁰ who obtain mostly three-particle-four-hole ($3p$ - $4h$) excitations in the ^{16}O closed shell for the structure of these levels. This is consistent with the fact that the positive-parity levels are seen strongly in the reaction $^{13}\text{C}(^3\text{He}, p)^{15}\text{N}$.²⁴ However, this reaction does not strongly populate the negative-parity states. The latter are seen strongly in the $^{12}\text{C}(\alpha, p)$ reaction at 22-MeV incident energy,²⁵ but the positive-parity levels at 9.05 and 10.07 MeV are extremely weak. The negative-parity states are also seen very strongly in reactions of ^6Li and ^7Li on ^{10}B and ^{11}B .²⁶ WCM calculations are not completely successful in describing these levels with $1h$ plus $2p$ - $3h$ and $4p$ - $5h$ configurations. They obtain very small $4p$ - $5h$ contributions to these states (also see the work of Shukla and Brown²⁷). The reaction data imply these levels may have strong overlap with configurations of a $p_{3/2}$ hole in the well-known 0^+ and 2^+ members of the deformed rotational band in ^{16}O at 6.05 and 6.92 MeV, respectively, which have large $4p$ - $4h$ strengths.²⁸

C. Higher Levels

The levels above 10-MeV excitation are not described by any model, and it is likely that their shell-model configurations are increasingly complex. Exceptions to this are the $T = \frac{3}{2}$ states at 11.61 and 12.52 MeV in ^{15}N . These are isobaric

analogs of the ^{15}C ground state and first excited state, and have a simple shell-model description as a $2s_{1/2}$ and $1d_{5/2}$ particle, respectively, outside a 0^+ , $T = 1$ core consisting of two holes in the $1p$ shell. This core corresponds to the ^{14}C ground state and ^{14}N first excited state at 2.31 MeV. Thus the ^{15}N states are seen strongly as resonances in the $^{14}\text{C} + p$ reaction. The $\frac{1}{2}^+$ state also has a large γ width for $E1$ decay to the $\frac{1}{2}^-$ ground state. The present experiment was performed to see how well the mirror correspondence persists between ^{15}N and ^{15}O at these high excitation energies and to identify the $T = \frac{3}{2}$ levels in ^{15}O which had not been seen but should lie within the region studied. At the latter, we were only partially successful.

The $^{14}\text{N}(p, p'\gamma)$ reaction to the 0^+ , $T = 1$ level at 2.31 MeV in ^{14}N would be expected to resonate at the $T = \frac{3}{2}$ levels, since it is isospin-allowed in the outgoing channel. However, the fact that the incoming channel is isospin-forbidden (the target has $T = 0$ and the projectile $T = \frac{1}{2}$), plus the fact that the resonances are expected to be broad, may make them difficult to observe above background. The

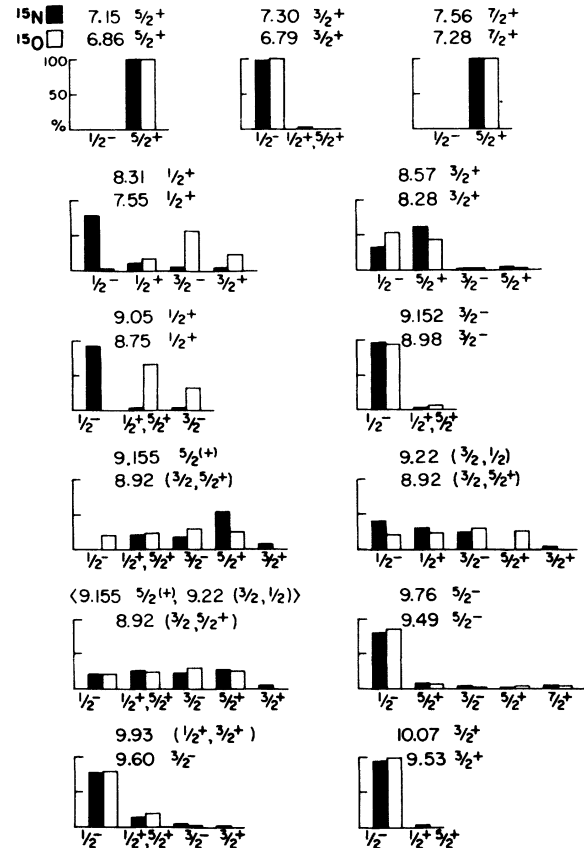


FIG. 7. Comparison of γ -ray branching ratios between mirror levels in ^{15}N - ^{15}O .

TABLE IV. ^{15}N γ -decay properties. See Refs. 9 and 10.

E_x (MeV)	E_x (MeV)	Branching ratio (%)	Γ_γ (eV)
11.61	0	91 ± 3	49
	5.30	7 ± 2	4
	6.32	2 ± 1	1
12.52	0	94 ± 1	4
	6.32	6 ± 1	0.3

$^{14}\text{N}(p, p'\gamma_{2,31})$ excitation function shows a strong, broad $\frac{1}{2}^+$ resonance at 10.94-MeV excitation energy and broad $\frac{3}{2}^+$ resonances at 11.75 and 12.12 MeV. A comparison of reduced widths and γ widths from Table III shows that appreciable $\frac{1}{2}^+$, $T = \frac{3}{2}$ strength lies in the 10.94-MeV level, but most of the particle strength is still unobserved in ^{15}O . Brill, Vongai, and Ogloblin²⁹ report a broad neutron group from the $^{13}\text{C}(^3\text{He}, n)$ reaction at 11.5 ± 0.1 -MeV excitation in ^{15}O which they believe is $T = \frac{3}{2}$, but such a state was not seen in the data of Adelberger and Nero³⁰ on the same reaction, nor is there evidence for such a state in any of the $^{14}\text{N} + p$ data.

Similarly, for the $\frac{5}{2}^+$, $T = \frac{3}{2}$ state there appears to be appreciable $T = \frac{3}{2}$ strength in both the 11.75- and 12.12-MeV levels in ^{15}O , but most of the single-particle strength seen in ^{15}N is still unobserved in ^{15}O . The γ -ray branching data in Table III also show no clear correspondence to the ^{15}N levels given in Table IV.

V. SUMMARY

The negative-parity levels of ^{15}O between 11 and 12.5 MeV can be seen to match up quite well to corresponding levels in ^{15}N , comparing their level sequence and spacings from Fig. 6 and their reduced partial widths in Table II. For the positive-parity levels in this region the picture is quite different. The $\frac{7}{2}^+$ level at 10.91 MeV in ^{15}O is probably the mirror of the high-angular-momentum level at 11.24 MeV in ^{15}N . The latter, because it is not far above threshold, is weakly excited as a resonance. Similarly, the $\frac{3}{2}^+$ level at 11.22 MeV in ^{15}O is probably the mirror of the level at 11.76 MeV in ^{15}N , although a large $E1$ γ strength to the ground state has been observed for the ^{15}O level but not the ^{15}N level. For the remaining levels, all of which probably have spin and parity of $\frac{1}{2}^+$ or $\frac{5}{2}^+$, the mirror correspondence appears to completely breakdown (see Table II). The $T = \frac{3}{2}$ strength in ^{15}O seems to be appreciably mixed into the $T = \frac{1}{2}$ levels of the same spin and parity, as might be expected because of the large widths of the $T = \frac{3}{2}$ states for the allowed decay to the ^{14}N 0^+ , $T = 1$ level at 2.31 MeV. The surprising fact, perhaps, is that there appears to be so little mixing of $T = \frac{3}{2}$ and $T = \frac{1}{2}$ levels in ^{15}N , in spite of the fact that there is a large overlap of both the $\frac{1}{2}^+$ and the $\frac{5}{2}^+$, $T = \frac{3}{2}$ levels with neighboring $T = \frac{1}{2}$ levels of the same spin and parity. (This phenomenon has led at least one author¹⁰ to suggest that the 12.49-MeV level in ^{15}N may not be $\frac{5}{2}^+$ but $\frac{7}{2}^+$.) Finally, it should be pointed out that the majority of the $T = \frac{3}{2}$ strength for both the $\frac{1}{2}^+$ and $\frac{5}{2}^+$ states is still unaccounted for in ^{15}O . This missing strength may lie in very broad levels underlying the states studied here and thus be difficult to observe above background via a $^{14}\text{N} + p$ reaction.

*Research supported in part by U. S. Atomic Energy Commission.

†Present address: Teledyne Isotopes, Westwood Laboratories, 50 Van Buren Avenue, Westwood, New Jersey 07675.

‡Schreiner Institute, Kerrville, Texas.

¹E. K. Warburton, J. W. Olness, and D. E. Alburger, Phys. Rev. **140**, B1202 (1965).

²A. E. Evans, B. Brown, and J. B. Marion, Phys. Rev. **149**, 863 (1966); A. E. Evans, *ibid.* **155**, 1047 (1967).

³G. W. Phillips, F. C. Young, and J. B. Marion, Phys. Rev. **159**, 891 (1967).

⁴F. Ajzenberg-Selove, Nucl. Phys. **A152**, 1 (1970).

⁵W. R. Harris and J. C. Armstrong, Phys. Rev. **171**, 1230 (1968).

⁶J. D. Henderson, E. L. Hudspeth, and W. R. Smith, Phys. Rev. **172**, 1058 (1968).

⁷J. K. Bair, H. O. Cohen, J. D. Kington, and H. B.

Willard, Phys. Rev. **104**, 1595 (1956).

⁸M. L. West, C. M. Jones, J. K. Bair, and H. B. Willard, Phys. Rev. **179**, 1047 (1969).

⁹H. M. Kuan, C. J. Umburger, and D. G. Shirk, Nucl. Phys. **A160**, 211 (1971); H. M. Kuan, private communication.

¹⁰F. C. Young, A. S. Figuera, and C. E. Steerman, Bull. Am. Phys. Soc. **15**, 522 (1970).

¹¹P. N. Shrivastava, F. Borelli, and B. B. Kinsey, Phys. Rev. **169**, 842 (1968).

¹²W. R. Wharton, P. von Brentano, W. K. Dawson, and P. Richard, Phys. Rev. **176**, 1424 (1968).

¹³H. M. Kuan, M. Hannoff, W. J. O'Connell, and S. S. Hanna, Nucl. Phys. **A151**, 129 (1970).

¹⁴J. B. Marion and F. C. Young, *Nuclear Reaction Analysis* (Wiley, New York, 1968).

¹⁵E. K. Warburton and J. W. Olness, Phys. Rev. **147**, 698 (1966).

¹⁶D. G. Shirk, S. Fiarman, N. Y. Wei, and H. M. Kuan, *Bull. Am. Phys. Soc.* **11**, 16, 489 (1971); H. M. Kuan, private communication.

¹⁷E. C. Halbert and J. B. French, *Phys. Rev.* **105**, 1563 (1957).

¹⁸A. P. Zuker, B. Buck, and J. B. McGrory, *Phys. Rev. Letters* **21**, 39 (1968).

¹⁹S. Lie, T. Engeland, and G. Dahll, *Nucl. Phys.* **156**, 449 (1970).

²⁰S. Lie and T. Engeland, to be published.

²¹A. Gallman, F. Jundt, E. Aslanides, and D. E. Alburger, *Phys. Rev.* **179**, 921 (1969).

²²B. Lawergren and I. V. Mitchell, *Nucl. Phys.* **A98**, 481 (1967).

²³G. W. Phillips and W. W. Jacobs, *Phys. Rev.* **184**, 1052 (1969).

²⁴C. E. Steerman and F. C. Young, *Bull. Am. Phys. Soc.* **15**, 529 (1970).

²⁵J. P. Allen and G. W. Phillips, Annual Report, Nuclear Physics Laboratory, University of Washington, Seattle, 1967 (unpublished), p. 37.

²⁶R. L. McGrath, *Phys. Rev.* **145**, 802 (1966).

²⁷A. P. Shukla and G. E. Brown, *Nucl. Phys.* **A112**, 296 (1968).

²⁸G. E. Brown and A. M. Green, *Nucl. Phys.* **25**, 401 (1966).

²⁹O. D. Brill, A. D. Vongai, and A. A. Ogloblin, *Izv. Akad. Nauk SSSR, Ser. Fiz.* **33**, 615 (1969) [transl.: *Bull. Akad. Sci. USSR, Phys. Ser.* **33**, 567 (1969)].

³⁰E. Adelberger and A. Nero, Progress Report, tandem Van de Graaff accelerator, Stanford University, 1968–1969 (unpublished), p. 44.

Two-Nucleon Interactions, the Unitary Model, and Polarization in Elastic Nucleon-Deuteron Scattering*

S. C. Pieper and K. L. Kowalski

Department of Physics, Case Western Reserve University, Cleveland, Ohio 44106

(Received 26 July 1971)

The use of the first-order unitary model to calculate nucleon polarizations in elastic nucleon-deuteron scattering at energies up to 40 MeV is investigated. One shortcoming of extant unitary-model calculations, that of inadequate two-nucleon input, is partially remedied by introducing a variety of more realistic models for the two-nucleon interaction. It is found that even with the latter interactions the unitary model fails to represent the nucleon polarization, and, as is to be expected from the work of Sloan *et al.*, to a lesser degree, the elastic differential cross section. The nucleon polarization is found to be extremely sensitive even at fairly low energies to the presence of the *P*-wave components of the two-nucleon amplitudes when the three-particle scattering is computed via the unitary and other approximations. This indicates that any method (exact or otherwise) for computing polarizations in *N-d* scattering must include these components.

I. INTRODUCTION

Recently calculations of the differential cross section and nucleon polarization in elastic nucleon-deuteron scattering were carried out over an energy range from 11 to 40 MeV using an approximate *K*-matrix formalism.¹⁻⁴ The results obtained were quite remarkable considering the crude two-nucleon input used and the approximations made to the three-particle dynamics. It now appears that the calculations of KK^{1,2} are incorrect.

The latter circumstance was first pointed out by Aarons and Sloan.⁵ Their primary (and correct) objection against the computational procedure in KK concerns a premature truncation in the total angular momentum *J*. However, even granting such a truncation ($J \leq \frac{3}{2}$) the results of KK appear to be unreproducible with the prescribed two-nucleon input.^{5,6} The computations to be described

in the present work substantiate the conclusions of Aarons and Sloan on both of these issues.

When sufficient partial-wave states are included to ensure convergence with respect to *J*, the *N-d* polarization predicted with the *N-N* interaction of KK is, as is shown in Ref. 5 and the present paper, essentially zero. In order to determine the cause of this complete disagreement with the experimental results, we have computed *N-d* polarizations and cross sections in the unitary model using a variety of more realistic *N-N* input. We conclude that even with a fairly complete representation of the *N-N* amplitudes (*S*, *P*, and *D* waves) the Sloan approximation fails to give qualitatively correct results for the *N-d* polarization. Although the structure of the elastic differential cross section is reasonably reproduced, the magnitude of the forward peak is, as is to be expected from the work of Sloan,⁴ poorly estimated.